

Resolver based Position Estimation of Vector Controlled PMSM Drive Fed by Matrix Converter

Sukanta Halder

Department of Electrical Engineering,
Indian Institute of Technology Roorkee,
Roorkee, India-247667
sukanta.raj@gmail.com

Pramod Agarwal

Department of Electrical Engineering,
Indian Institute of Technology Roorkee,
Roorkee, India-247667

Anubhav Agrawal

Department of Electrical Engineering,
Indian Institute of Technology Roorkee,
Roorkee, India-247667

S.P. Srivastava

Department of Electrical Engineering,
Indian Institute of Technology Roorkee,
Roorkee, India-247667

Abstract—This paper proposes resolver based position estimation for matrix converter fed permanent magnet synchronous motor (PMSM) drive. A matrix converter fed PMSM drive replaces the conventional voltage-source inverter (VSI) drive due to its advantageous feature like elimination of bulky and life limited dc-link capacitors, inherent bidirectional power flow, the sinusoidal input current drawn and controllable input power factor. The ZDAC control is implemented to achieve the independent control of speed and torque in PMSM drive. High frequency signal is applied to excite the resolver primary winding. Demodulation based algorithm is implemented to calculate the speed and rotor position. Feedback loop control is used to compute the rotor position from the resolver. The accurate position is estimated without using resolver to digital converter. The dynamic performance of proposed drive is simulated in Matlab/Simulink environment under load variation.

Keywords- Permanent Magnet Synchronous Motor; Resolver; Matrix Converter; AC-AC Converter; Zero d-axis current control; Vector control. RDC

I. INTRODUCTION

The advancement of electric motor drive creates revolution in the industrial world. With the advanced feature like High power density and efficiency, high torque to inertia ratio and high reliability PMSM becomes the favorites in the variable speed drive. In the past most of the industrial application were based on the voltage source inverters (VSI) based drive. But the advantageous feature like high power density, sinusoidal input/output currents, bi-directional energy flow capability and controllable input power factor and high power/volume ratio because of the absence of a DC link filter, attracts the researcher to work with Matrix converter fed PMSM drive [1-6]. To implement the ZDAC control the information of the rotor position is necessary. Resolver sensor basically provides the rotor position. Robust structure and noise insensitivity are the attracting features of this sensor [7, 8].

The literatures [7-14] provide the information regarding the resolver sensor. But RDC less implementation with complete drive system is still attracting area for the researchers. A bang-hang type phase comparator is implemented for fast tracking. Two pre-filters outside the R/D conversion loop are used as low pass filter [10]. By proper processing of the two resolver output signal sine and cosine, the reasonably accurate angle measurement is done by dedicated compensation method without a processor and/or a look-up table [11].

Duty cycle optimization based direct torque control strategy has been presented for MC in [3]. Different switching states of matrix converter including the rotation vectors have been described [4]. Reduction in the current harmonic of PMSM has been observed with adjusting a pseudo dc bus voltage. The switching strategy based on back-propagation neural network is used to adjust this voltage [5]. Smooth control of torque and flux with fixed switching frequency achieved with master and slaves vectors in [6]. A nonlinear adaptive back stepping controller has been presented [15]. This controller can track a time-varying speed command and a time-varying position command. Use of MC input voltages with different amplitudes has been investigated in [16] which reduce the inherent torque ripple with direct torque control of PMSM.

In this paper the demodulation based resolver algorithm with ZDAC control of PMSM drive has been simulated. Instead of conventional VSI, Matrix converter has been used to fed the motor. The position estimation has been done without using RDC. The Vector controller has been designed in terms of ZDAC control strategy. The dynamic performance of the drive for load varying condition has been simulated.

II. MATRIX CONVERTER

The MC is based on high synthesis control of input AC voltage which converts fixed AC voltage and frequency into variable voltage and variable frequency [17, 18]. It is an array of bi-directional switches which connects 'm' input phase to 'n' output phase. In general, a 3x3 structure of matrix converter comprises of 9 bi-directional switches as shown in Figure 1.

The presence of bi-directional switches makes the converter operational in all the 4 quadrants. But, at the same time the scarcity of the availability of packed bi-directional switches has hindered the application of MC in industry at a large scale. MC has been able to replace the existing 2 stage AC-DC-AC conversion scheme used in variable frequency drives. In the present study, Modified Venturini Algorithm is used for switching the MC [19]. The reference I_d and I_q values are set by passing the speed error from speed Proportional Integral (PI) controller. The reference voltages for the controller are calculated by processing the current error through PI controller.

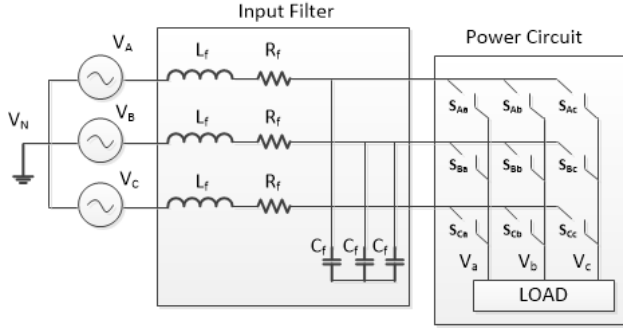


Figure 1. Schematic diagram Matrix Converter.

The mathematical equations for the output voltage are given as:

$$V_{rs} = qV_{im} \cos(\omega_o t) - \frac{q}{6}V_{im} \cos(3\omega_o t) + \frac{1}{4}V_{im} \cos(3\omega_i t) + \text{harmonics} \quad (1)$$

$$V_{ys} = qV_{im} \cos(\omega_o t + \frac{2\pi}{3}) - \frac{q}{6}V_{im} \cos(3\omega_o t) + \frac{1}{4}V_{im} \cos(3\omega_i t) + \text{harmonics} \quad (2)$$

$$V_{bs} = qV_{im} \cos(\omega_o t + \frac{4\pi}{3}) - \frac{q}{6}V_{im} \cos(3\omega_o t) + \frac{1}{4}V_{im} \cos(3\omega_i t) + \text{harmonics} \quad (3)$$

These voltages can be transformed to d-q reference frame rotating at a synchronous electrical angular velocity of the fundamental component of voltage applied to the machine stator (i.e., ω_e). The transformed voltages can be written as:

$$V_{qs} = V_o [1 - \frac{1}{6} \cos(\omega_e t) \cos(3\omega_e t) + \frac{1}{4q} \cos(\omega_e t) \cos(3\omega_i t) + \text{harmonics}] \quad (4)$$

$$V_{ds} = V_o [-\frac{1}{6} \cos(\omega_e t) \cos(3\omega_e t) + \frac{1}{4q} \cos(\omega_e t) \cos(3\omega_i t) + \text{harmonics}] \quad (5)$$

III. THE RESOLVER AND POSITION ESTIMATION

Construction wise resolver has three winding, one primary and two secondary. The primary winding is fixed on the rotor and two secondary stationary coils are placed in 90° shifted with one another. The principle of operation of a resolver sensor is like a transformer. The primary coil is excited by high frequency signal. Corresponding to the excitation two secondary will produce sine and cosine signal as shown in the Figure 2.

The equations relating with the primary and secondary winding are defined as –

$$V_{in}(t) = \hat{V}_{in} \cdot \sin \omega_{ref} t \quad (6)$$

$$V_{o1}(\phi, t) = \hat{V}_{in} \cdot k \cdot \sin \phi \cdot \sin \omega_{ref} t \quad (7)$$

$$V_{o2}(\phi, t) = \hat{V}_{in} \cdot k \cdot \cos \phi \cdot \sin \omega_{ref} t \quad (8)$$

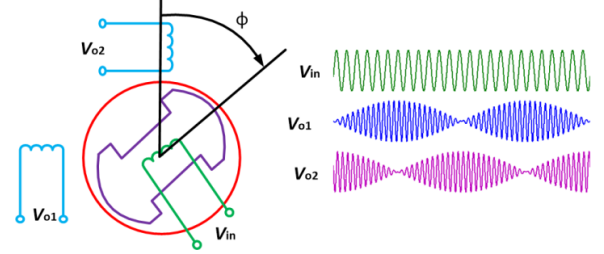


Figure 2. Resolver construction and operation

Where, k is the resolver's turn ratio, \hat{V}_{in} implies the peak value, ϕ is the rotor position in rad., and ω_{ref} is the frequency of the excitation signal in (rad./sec.).

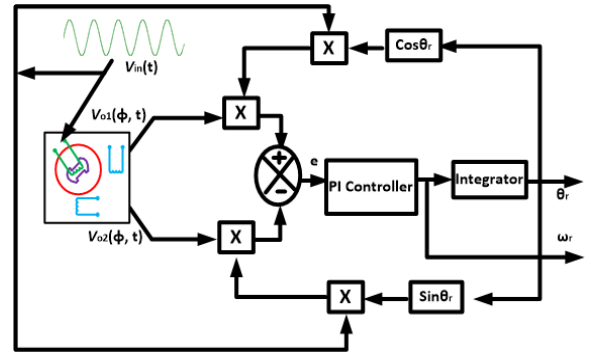


Figure 3. Schematic diagram of resolver algorithm

The feedback loop and PI controller provides the speed. The rotor position is obtained by integration of the motor speed.

The error calculation is based on following trigonometric relation-

$$e = (\hat{V}_{in} \cdot \sin \omega_{ref} t \cdot \cos \theta) (\hat{V}_{in} \cdot k \cdot \sin \phi \cdot \sin \omega_{ref} t) - \quad (9)$$

$$(\hat{V}_{in} \cdot \sin \omega_{ref} t \cdot \sin \theta) (\hat{V}_{in} \cdot k \cdot \cos \phi \cdot \sin \omega_{ref} t)$$

$$e = \hat{V}_{in}(t) \cdot (\hat{V}_{in} k \cdot \sin \omega_{ref} t) (\sin \phi \cos \theta - \cos \phi \sin \theta) \quad (10)$$

The above expression can be written in form of-

$$e = A \cdot \sin(\phi - \theta) \quad (11)$$

Where,

$$A = \hat{V}_{in}(t) \cdot (\hat{V}_{in} k \cdot \sin \omega_{ref} t) \quad (12)$$

IV. PROPOSED DRIVE SYSTEM

The control process is implemented for the proposed drive in d-q reference frame, because in d-q reference frame quantities are independent and can be controlled separately

which is the basic purpose of the vector control. The stator voltage equations are:

$$V_{qs}^r = r_q i_{qs}^r + p \lambda_{qs}^r + \omega_r \lambda_{ds}^r \quad (13)$$

$$V_{ds}^r = r_d i_{ds}^r + p \lambda_{ds}^r - \omega_r \lambda_{qs}^r \quad (14)$$

$$V_{0s}^r = r_s i_{0s}^r + p \lambda_{0s}^r \quad (15)$$

where r_q and r_d are the q-axis and d-axis winding resistance. V_{qs}^r and V_{ds}^r are the q and d-axis voltage in the rotor reference frame. i_{qs}^r and i_{ds}^r are the q and d-axis current. The flux linkages are

$$\lambda_{qs}^r = L_q i_{qs}^r \quad (16)$$

$$\lambda_{ds}^r = L_d i_{ds}^r + \lambda_m^r \quad (17)$$

By considering constant magnet flux linkage $p \lambda_m^r = 0$

$$V_{qs}^r = (r_s + p L_q) i_{qs}^r + \omega_r L_d i_{ds}^r + \omega_r \lambda_m^r \quad (18)$$

$$V_{ds}^r = (r_s + p L_d) i_{ds}^r - \omega_r L_q i_{qs}^r \quad (19)$$

The electromagnetic torque can be given by

$$T_e = \frac{3}{2} \cdot \frac{P}{2} (\lambda_{ds}^r i_{qs}^r - \lambda_{qs}^r i_{ds}^r) \quad (20)$$

Which upon substitution of the flux linkages in terms of the inductance and current

$$T_e = \frac{3}{2} \cdot \frac{P}{2} \{ (\lambda_m^r i_{qs}^r + (L_d - L_q) i_{ds}^r i_{qs}^r) \} \quad (21)$$

The equivalent circuit diagram of PMSM for q-axis and d-axis is shown in Figure 4. (a) and (b) respectively.

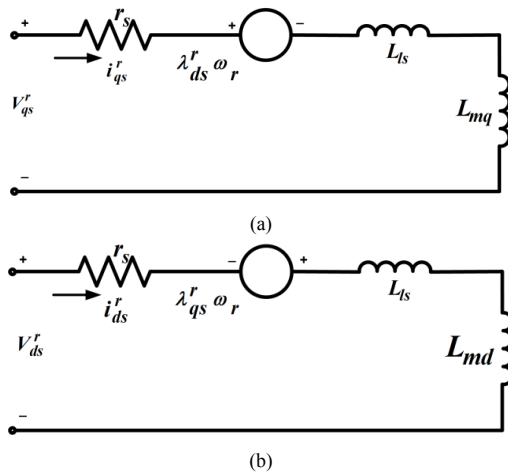


Figure 4. Equivalent circuit of PMSM (a) q-axis, (b) d-axis.

In ZDAC the torque angle is maintained constant at 90 degrees.

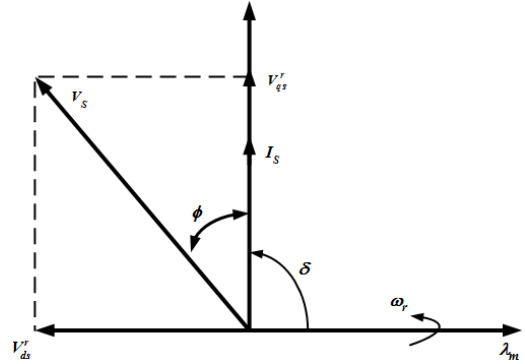


Figure 5. Constant torque-angle or Zero d-axis control phasor diagram

In the industrial application ZDAC is used due to its simple operation. The d-axis current is maintained at zero. The main advantage of ZDAC control strategy is that it simplifies the current control.

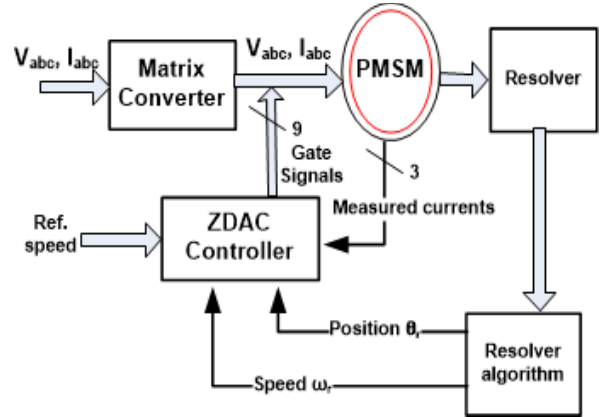


Figure 6. Block diagram of ProposedMC fed PMSM drive with Resolver sensor

As the q axis current become the function of torque value. If the d axis current made equal to zero

$$i_{ds}^r = 0 \quad (22)$$

By putting this value in equation for electromagnetic torque we can get

$$T_e = \frac{3}{2} \cdot \frac{P}{2} \lambda_m^r i_{qs}^r \quad (23)$$

Rewriting this equation it can be seen that q axis current become a function of torque.

$$i_{qs}^r = \frac{T_e}{\left(\frac{3}{2}\right) \cdot \left(\frac{P}{2}\right) \lambda_m^r} \quad (24)$$

Figure 6. shows the block diagram of the proposed drive scheme. Reference i_{qs}^* current is generated from the torque and i_{ds}^* make equal to zero. The reference torque value is generated based on the speed error. The current errors are processed through PI controllers to obtain the voltage reference signal for Modified Venturini control.

V. SIMULATION RESULT

Output signal of resolver at complete 360° rotation of the rotor shaft is shown in the Figure 7. It is observed that the Sine output signal is zero and the cosine signal is in phase with the input signal at the starting position when the angle is zero. Trace 1 represents the input high frequency excitation signal of the resolver. Trace 2 and 3 represents the modulated sine & cosine output signal of the resolver.

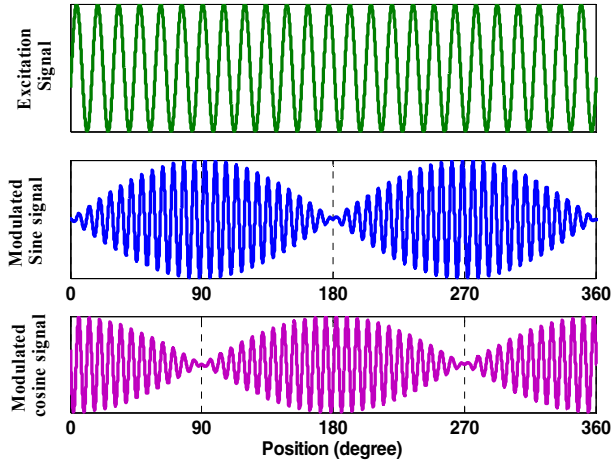


Figure 7. Simulation results of the resolver input and Modulated output signal with complete 360° rotation.

The proposed drive scheme is simulated in Matlab environment with variation in load torque. The specifications of the PMSM used in the study are listed in Table I.

TABLE I. SPECIFICATION OF SIMULATED MOTOR

stator phase resistance	2.55 Ω
Torque Constant	0.75Nm/A
Phase inductance	5.15mH
Moment of inertia (J)	0.000062kg-m ²
Total load inertia	0.001914 kg-m ²
No of poles	8
Damping friction	0.0041N-m/rad

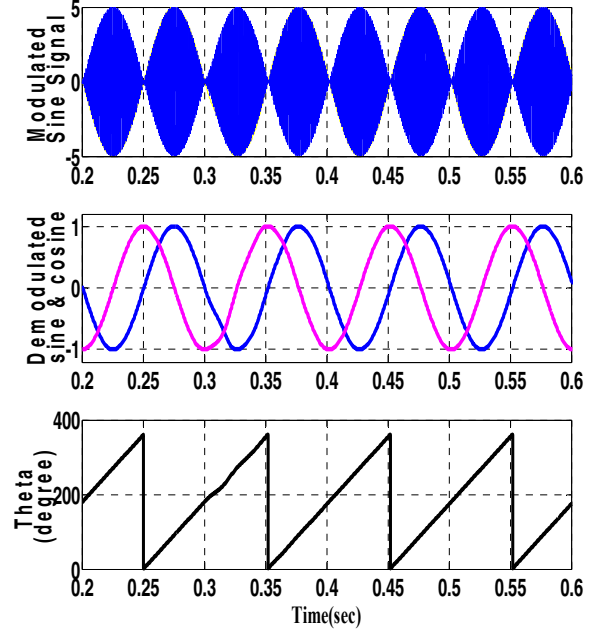
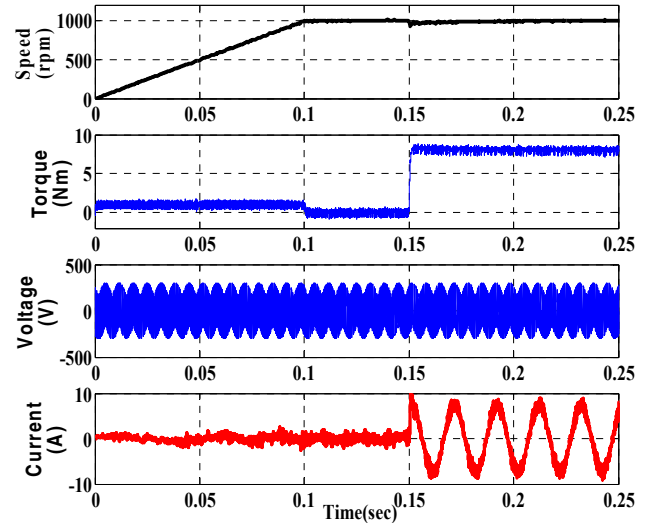


Figure 8. Simulation results of demodulated and modulated output signal and position of the rotor shaft.

The high frequency (1 kHz) excitation signal is applied to the resolver. When the rotor is rotated, the resolver induces the two modulated signals. To obtain the rotor position from the resolver, these modulated signals are demodulated by the proposed algorithm. Trace 1 in the Figure 8. denotes the modulated output sine signal & the trace 2 denotes the demodulated sine and cosine signal. Trace 3 in the Figure 8. shows the estimated position from the resolver algorithm.



(a)

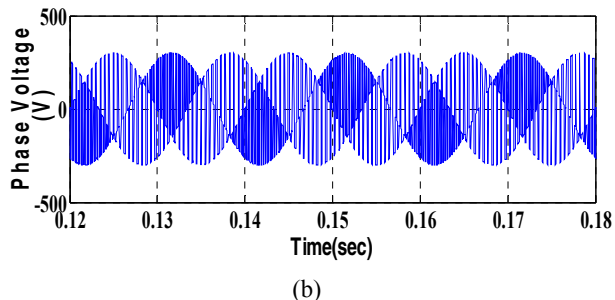


Figure 9. (a) Dynamic response of PMSM drive at load variation. (b) Magnified view of phase voltage.

The dynamic response of the machine is shown in Figure 9. The motor is started with a reference slope so as to minimize the starting current. At 0.15 seconds, 8 Nm load is applied to the machine. It is clear from the figure that with the application of load torque, there is a dip in the machine speed which is adjusted to the reference value by the proposed closed loop control operation. The magnified view of the phase voltage is shown in the Figure 9. (b).

VI. CONCLUSION

In this present study, the resolver based position estimation has been done by demodulating the output signal. Accurate position estimation has been achieved. Modulated Output signals of resolver at complete 360° rotation of the rotor shaft have been presented. With the variation of rotor position the modulated output signal also changes. The performance of MC fed PMSM drive is evaluated. Vector control in terms of zero d-axis current control has been implemented in PMSM. The closed loop operation is achieved using the actual rotor position estimated from the resolver algorithm. With the application of MC, the drive can operate at unity power factor. It has been observed that Matrix converter can replace the conventional VSI for industrial application.

REFERENCES

- [1] Bouchiker, S., Capolino, G.A. and Poloujadoff, M. (1998), "Vector Control of a Permanent-magnet Synchronous Motor using AC-AC Matrix Converter", in *IEEE Transactions on Power Electronics*, Vol. 13, No. 6, pp. 1089–1099, Nov 1998.
- [2] Nalepa, R. and Orłowska-Kowalska, T. (2012), "Optimum Trajectory Control of the Current Vector of a Nonsalient-pole PMSM in the Field-weakening Region", *IEEE Trans. Ind. Electron.*, Vol. 59, No. 7, pp. 2867–2876, Jul. 2012.
- [3] Xia, C., Zhao, J., Yan, Y. and Shi, T. (2014), "A Novel Direct Torque Control of Matrix Converter-Fed PMSM Drives Using Duty Cycle Control for Torque Ripple Reduction", in *IEEE Transactions on Industrial Electronics*, Vol. 61, No. 6, pp. 2700–2713, June 2014.
- [4] Xia, C., Zhao, J., Yan, Y. and Shi, T. (2014), "A Novel Direct Torque and Flux Control Method of Matrix Converter-Fed PMSM Drives", in *IEEE Transactions on Power Electronics*, Vol. 29, No. 10, pp. 5417–5430, Oct. 2014.
- [5] Chen, Der-Fa and Liu, Tian-Hua (2003), "Optimal Controller Design for a Matrix Converter based Surface Mounted PMSM Drive System", in *IEEE Transactions on Power Electronics*, Vol. 18, No. 4, pp. 1034–1046, July 2003.
- [6] Yan, Y., Zhao, J., Xia, C. and Shi, T. (2015), "Direct Torque Control of Matrix Converter-fed Permanent Magnet Synchronous Motor Drives based on Master and Slave Vectors", in *IET Power Electronics*, Vol. 8, No. 2, pp. 288–296.
- [7] Pillay, P. and Krishnan, R. (1989), "Modeling, Simulation and Analysis of Permanent-magnet Motor Drives I. The Permanent-magnet Synchronous Motor Drive", in *IEEE Transactions on Industry Applications*, Vol. 25, No. 2, pp. 265–273, Mar/Apr 1989.
- [8] Hou, C.C., Chiang, Y.H. and Lo, C.P. (2014), "DSP-based Resolver-to-digital Conversion System Designed in Time Domain", in *IET Power Electronics*, Vol. 7, No. 9, pp. 2227–2232, September 2014.
- [9] Hanselman, D.C. (1991), "Techniques for Improving Resolver-to-digital Conversion Accuracy", *IEEE Trans. Ind. Electron.*, Vol. 38, No. 6, pp. 501–504, Dec. 1991.
- [10] Yim, C.H., Ha, I.J. and Ko, M.S. (1992), "A Resolver-to-digital Conversion Method for Fast Tracking", *IEEE Trans. Ind. Electron.*, Vol. 39, No. 5, pp. 369–378, Oct. 1992.
- [11] Benammar, M., Ben-Brahim, L. and Alhamadi, M.A. (2004), "A Novel Resolver-to-360° Linearized Converter", *IEEE Sensors J.*, Vol. 4, No. 1, pp. 96–101, Feb. 2004.
- [12] Hoseinnezhad, R. (2006), "Position Sensing in Brake-by-wire Callipers using Resolvers", *IEEE Trans. Veh. Technol.*, Vol. 55, No. 3, pp. 924–932, May 2006.
- [13] Attaianesi, C. and Tomasso, G. (2007), "Position Measurement in Industrial Drives by Means of Low-Cost Resolver-to-Digital Converter," in *IEEE Transactions on Instrumentation and Measurement*, Vol. 56, No. 6, pp. 2155–2159, Dec. 2007.
- [14] Murakami, S., Shiota, T., Ohto, M., Ide, K. and Hisatsune, M. (2012), "Encoderless Servo Drive with Adequately Designed IPMSM for Pulse-Voltage-Injection-Based Position Detection", in *IEEE Transactions on Industry Applications*, Vol. 48, No. 6, pp. 1922–1930, Nov.-Dec. 2012.
- [15] Liu, T.H., Chen, D.F. and Hung, C.K. (2005), "Nonlinear Controller Design and Implementation for a Matrix-converter-based PMSM Drive System", in *IEEE Proceedings-Electric Power Applications*, Vol. 152, No. 5, pp. 1037–1048, 9 Sept. 2005.
- [16] Ortega, C., Arias, A., Caruana, C., Balcells, J. and Asher, G. (2010), "Improved Waveform Quality in the Direct Torque Control of Matrix-converter-fed PMSM Drives", *IEEE Trans. Ind. Electron.*, Vol. 57, No. 6, pp. 2101–2110, Jun. 2010.
- [17] Wheeler, P. et al. (1994), "A Theoretical and Practical Consideration of Optimised Input Filter Design for a Low Loss Matrix Converter", in *9th International Conference on Electromagnetic Compatibility*, pp. 138–142.
- [18] Wheeler, P.W. et al. (2002), "Matrix Converters: A Technology Review", *IEEE Transactions on Industrial Electronics*, Vol. 49, pp. 276–288.
- [19] Altun, H. and Sünter, S. (2003), "Matrix Converter Induction Motor Drive: Modeling, Simulation and Control", *Electrical Engineering*, Vol. 86, pp. 25–33.